The 18th Scandinavian International Conference on Fluid Power, SICFP'23, May 30- June 1, 2023, Tampere, Finland

A novel framework for the estimation of excavator's actual productivity in the grading operation using building information modeling (BIM)

Amirmasoud Molaei[1,2], Marcus Geimer[1], and Antti Kolu[2]

[1]Institute of Mobile Machines, Karlsruhe Institute of Technology, Karlsruhe, Germany
[2]Radical Innovation Research Group, Novatron Ltd., Pirkkala, Finland
E-mail: amirmasoud.molaei@partner.kit.edu, marcus.geimer@kit.edu, antti.kolu@novatron.fi

Abstract

This paper discusses the productivity of an excavator in the grading operation. Although the grading operation is one of the most important tasks in various worksites, there is no automated algorithm to calculate the excavator's productivity during the grading operation. Manual methods for measuring the height of ground are highly time-consuming, labor-intensive, and error-prone. In the presented method, a height map from surrounding areas is provided using a light detection and ranging (LiDAR) sensor every few seconds. The proposed approach utilizes building information modeling (BIM) to retrieve information about the desired shape of the surface and the required accuracy. The results of the presented method are shown by implementation on a collected dataset using an excavator.

Keywords: Excavator's productivity, grading operation, elevation terrain mapping, building information modeling (BIM).

1 Introduction

Heavy-duty mobile machines (HDMMs) play significant roles in the world and are utilized in many industries such as construction, forestry, and mining industries. The industries are highly increasing and have significant challenges such as skilled labor shortage, harsh work environments, and low productivity. HDMMs significantly impact the productivity and efficiency of various construction projects [1,2]. It has been studied that approximately 40% of direct costs in highway construction projects are related to the HDMMs. Thus, improving the productivity of HDMMs can be an appropriate answer to the challenges [3].

There is a common quote about work performance evaluation and monitoring that says 'If you cannot measure it, you cannot improve it' [4]. Traditional manual productivity monitoring highly depends on manual data collection that is extremely time-consuming, highly-priced, and error-prone [5]. Accurate and precise monitoring of the earth-moving operations under different working conditions is highly required and is an important step toward semi and fully-autonomous HDMMs [6]. Not only monitoring the machines' productivity can reduce the operation time, fuel consumption, and costs, but also can optimize the planning and working parameters, discover potential project issues, and improve the management and economic situations [3, 7].

1.1 Hydraulic Excavator

There are different types of HDMMs, and the hydraulic excavator is one of the most significant pieces of equipment in the construction industry. Almost all construction projects such as the construction of highways, airports, industrial and residential buildings need different types of excavation work. An excavator is a multi-functional machine that is utilized for different earth-moving operations because it can perform different tasks such as digging, trenching, and grading [6]. An excavator is a human-operated machine that is mostly driven using a hydraulic system. During different operations, human operators utilize their sense and reasoning-based knowledge to control and monitor the operation. A typical hydraulic excavator is shown in Fig. 1. The traveling body, swing body, and front digging manipulator are three main parts of an excavator. The boom, arm, and bucket build the manipulator of the machine. Also, an excavator has three revolute joints between the swing body, boom, arm, and bucket [8].

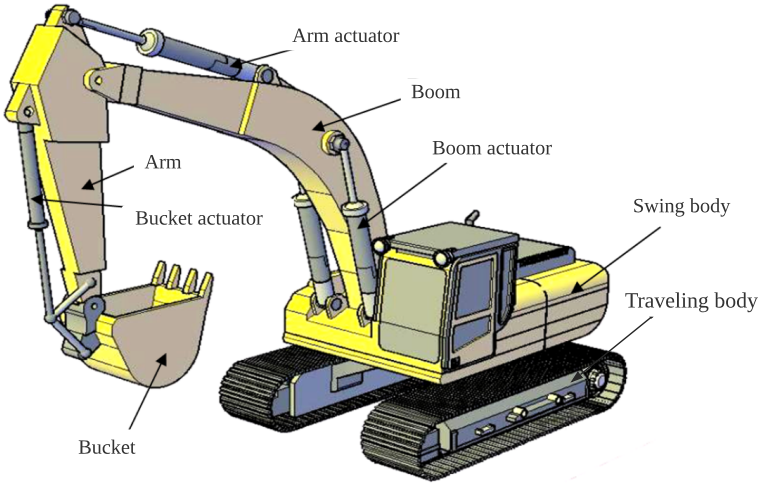

Figure 1: A typical hydraulic excavator and its different parts [3].

1.2 Grading Operation

Estimating the productivity of HDMMs in earth-moving tasks is a major challenge. The productivity of the excavator must be defined based on the goals of the working cycle. A grading operation involves using an excavator to level and smooth the surface of the ground. This is typically done for construction or landscaping purposes, to prepare a site for building, or to create a flat, even surface for paving or other purposes. The excavator uses its bucket to move and spread the material to create a level surface. The grading operation by using an excavator is depicted in Fig. 2. Although the grading operation is one of the essential and common tasks in various projects, it is highly challenging for operators. Since the grading task needs the simultaneous manipulation of the boom, arm, and bucket cylinders in the excavator. Also, compared to other excavation tasks, the grading operation needs much higher positioning accuracy within ± 5 or ± 10 *cm*. Nowadays, several advanced algorithms have been developed for automated grading operations that assist less experienced operators in swiftly and accurately completing tasks. The type of material, the shape of the desired surface, the required accuracy, the size of the bucket and excavator, weather conditions, and the skills of human operators are influencing factors that can significantly change the productivity of the excavator in the grading operation [5]. Generally, the quantity of material and the operation cycle time are the essential parameters for the productivity of most cyclical types of machinery. The quantity of transferred material per unit of time is the simplest definition of the excavator's productivity; nevertheless, this definition cannot be beneficial for the productivity calculation of the grading operation. In the grading operation, the quality and time of the operation have the highest priority for worksite managers, and only a small amount of materials are added or removed. Thus, the quantity of material cannot illustrate the actual productivity of the operation. In this paper, the area of the graded surface per unit of time is used as a meaningful productivity definition for the grading operation:

$$Q = \frac{A}{T} \tag{1}$$

where Q is the productivity $[m^2/sec]$, A is the area of the graded surface $[m^2]$, and T is the time $[sec]$.

Figure 2: The grading operation using an excavator [9].

1.3 Literature Review

During the last 20 years, several academic and commercial automated excavating techniques have been developed [10–14]. Notwithstanding, there is no automated method to measure the productivity of an excavator in the grading operation. In traditional methods, a surveyor prepares data for measuring the progress and conducts surveys on construction sites. But nowadays, 3D technology can be a promising solution to challenges in construction sites. In [15], depth differences in terrain are calculated using a light detection and ranging (LiDAR) sensor to determine the excavation changes. Sometimes the sensor vision is blocked due to obstacles such as piles that can decrease the accuracy of volume estimation. In [16], two methods for ground volume estimation based on LiDAR measurements are implemented and compared. In [17], an integrated vision and control system is presented that enables a robot to navigate through rough terrain with obstacles. The occluded parts of terrains are reconstructed by applying point-cloud matching and non-parametric terrain modeling techniques. In [18], a 3D visualization technique for a construction site is proposed based on a stereo camera and a LiDAR sensor. In [19], a method is described for automatically estimating the excavation volume needed for road widening from point cloud data collected by a laser mobile mapping system (LMMS). In [20], a network-based cloud system for managing soil volume progress on a construction site is suggested. The daily progress volume is determined utilizing bucket cutting-edge historical data that was obtained from sensors installed on heavy equipment. In [6], three elements of efficient excavation progress monitoring: calculation of the excavation volume, identification of occlusion zones, and 5D mapping are addressed. The component for determining excavation volume allows for both bucket volume and ground excavation volume estimation. In [21], three surveying techniques in the mining industry, photogrammetry, terrestrial laser scanning (TLS), and aerial laser scanning (ALS), are compared and evaluated based on time consumption, efficiency, and safety. Additionally, a coordinate-based volumetric computational approach is developed to estimate the volume of stockpiles using LiDAR data obtained from a laser scanner. In the literature review, the main focus is on the quantity of the material. However, in landscaping tasks, particularly the grading task, the quality and accuracy of the operation have the highest priority and must be taken into account. Furthermore, although building information modeling (BIM) has a high potential to improve the performance of various earth-moving operations, no approach is presented to use its potential in productivity estimation algorithms.

1.4 Objectives

In this paper, a new algorithm is proposed to measure the area of the graded surface per unit of time based on the target model obtained from BIM as the actual productivity of the excavator in the grading operation. An elevation terrain mapping algorithm is utilized to model surrounding areas by using a LiDAR sensor on top of the excavator. Since the movements of the bucket, arm, and boom in front of the excavator add extra points to the point cloud, the positions of revolute joints are estimated to be able to remove the extra points from the point cloud. The positions of the bucket, arm, and boom are estimated based on the measurements of inertial measurement units (IMUs) and forward kinematics of the excavator. In addition, the shape of the desired surface is provided by BIM. To estimate the actual productivity of the excavator, the difference between the actual map and the desired surface should be less than the required accuracy. It has been assumed the error between the initial terrain and the target surface is less than the bucket's height, and no digging operation is needed before the grading operation. The proposed method for the productivity estimation of the grading operation can provide a useful measure to evaluate manual or automated grading operations. Finally, the presented method is implemented on a collected dataset using an excavator in a private worksite. The results show that the presented method can efficiently monitor the excavator's productivity in the grading operation.

The remainder of this paper is outlined as follows. Section 2 describes the presented method for the actual productivity estimation of an excavator in the grading operation. This section consists of three main parts: (1) elevation terrain mapping algorithm, (2) building information modeling (BIM), and (3) productivity estimation. The data collection step is explained in Section 3. Results are presented in Section 4. Finally, Section 5 concludes the paper.

2 Methodology

2.1 Elevation terrain mapping

In the proposed method, a height map from surrounding environments is required to calculate the excavator's productivity in the grading operation. Measurements of sensors such as LiDAR, stereo cameras, and RADARs are combined with localization data from the global navigation satellite system (GNSS), IMUs, or wheel odometry to build the map. An elevation map is a typical data structure for depicting the surrounding areas of a robot. In a grid-based height map (2.5D map), each cell shows the height of the terrain within the cell relative to some known reference value, such as elevation above sea level. The accuracy of the map in the global frame highly depends on the accuracy of the localization data and sensor calibration [17].

Nowadays, the LiDAR sensor is one typical piece of mapping equipment. To establish the 3D point cloud of spatial data, measurements are transformed from the Spherical coordinate of the sensor into the global Cartesian coordinate system. When the real location and orientation of the LiDAR sensor diverge from the measured values, the transformation is prone to errors. In most cases, a series of transformations, such as from the sensor coordinate frame to the machine's body frame and further into a global frame, should be applied to generate the final elevation map. Small errors in transformations accumulate and bring about huge errors in the final map [22].

2.1.1 Transformation

The measurements of LiDAR are provided in the sensor coordinate system. The data should be transformed into point clouds in a global Cartesian coordinate system in order to be used for mapping. A sequence of coordinate transformations is required to accomplish this. The frames $A_i \in \{g, m, s\}$ involve coordinate transformations. These frames are the global (g), machine (m), and sensor (s) frames. An affine coordinate transformation is formalized by Eq. (2):

$$\begin{aligned} {}^{j}T_i &= \begin{bmatrix} {}^{j}R_i & {}^{j}P_i \\ 0_{1\times 3} & 1 \end{bmatrix} \\ {}^{j}R_i({}^{j}\varphi_i, {}^{j}\theta_i, {}^{j}\psi_i) &= R_{roll}({}^{j}\varphi_i) R_{pitch}({}^{j}\theta_i) R_{yaw}({}^{j}\psi_i) \\ {}^{j}P_i &= [{}^{j}x_i, {}^{j}y_i, {}^{j}z_i]^T \end{aligned} \tag{2}$$

where ${}^{j}T_i$ is the 4 by 4 transformation matrix from i_{th} frame to j_{th} frame, ${}^{j}R_i$ is the 3 by 3 rotation matrix, ${}^{j}P_i$ is the 3 element translation vector, $R_{roll}({}^{j}\varphi_i)$ is the rotational matrix around x-axis, $R_{pitch}({}^{j}\theta_i)$ is the rotational matrix around y-axis, $R_{yaw}({}^{j}\psi_i)$ is the rotational matrix around z-axis, and ${}^{j}\varphi_i$, ${}^{j}\theta_i$, and ${}^{j}\psi_i$ are the roll, pitch and yaw angles, respectively [22].

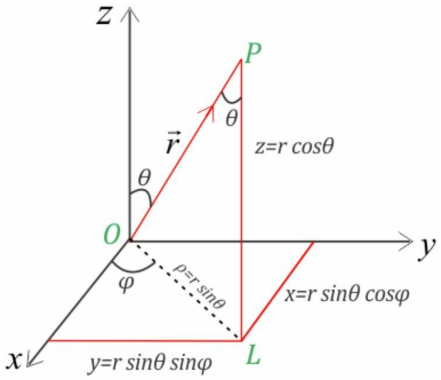

Figure 3: Relationship between Spherical and Cartesian coordinates [23].

A single LiDAR measurement can be expressed as Spherical coordinates (r, θ, ϕ) or Cartesian coordinates (x, y, z). The relationship between Cartesian and Spherical coordinates is shown in Fig. 3. The point ${}^{s}P$ in the sensor frame is transmitted to a point ${}^{g}P$ in the global frame using the chain of transformations

$${}^{g}P = {}^{g}T_m {}^{m}T_s {}^{s}P, \tag{3}$$

where ${}^{m}T_s$ is the sensor frame to machine frame transformation and ${}^{g}T_m$ is the machine frame to global frame transformation. ${}^{m}T_s$ is determined based on target-based sensor-to-machine calibration techniques. In target-based calibration, known targets are used to provide reference points for aligning the sensor and the machine. The target can be any object with well-defined, known dimensions and a known location relative to the machine frame. Target-based calibration can be highly useful because it allows for precise alignment between the sensor and the machine frame using known reference points [24]. ${}^{g}T_m$ is estimated using the Extended Kalman Filter (EKF) with GNSS, accelerometer, and gyroscope data. An EKF is widely used for combining measurements from multiple sensors to estimate the state of a system. The first step is to define the machine's position as state variables in the EKF. The next step is to collect measurements from the GNSS and IMU. The GNSS provides measurements of the machine's position (latitude, longitude, and altitude), and the IMU provides measurements of the machine's acceleration and angular velocity. Based on the state variables and the previous sensor measurements, the EKF uses a mathematical model to predict the current state of the machine. This prediction is called the 'a priori' estimate. The EKF then compares the priori estimate with the current sensor measurements to produce the 'a posteriori' estimate. This process is called the measurement update, and it involves using the Kalman gain to weigh the relative contributions

of the priori estimate and the sensor measurements. The process of predicting and updating the states is repeated at regular intervals using the latest sensor measurements. Overall, the EKF provides a powerful tool for combining GNSS and IMU measurements to estimate the states of a machine in a global coordinate system [25].

A height map consists of a two-dimensional grid in which each cell stores the mean and variance of height. The height map is produced by assigning each point in the 3D point cloud to a cell based on their x and y coordinates. The z coordinate values of all 3D points allocated within a cell are considered new measurements of the cell. The previous estimation of the height in a cell is then updated using the new measurements according to a Bayesian update technique. In our algorithm, the forgetfulness scheme [26] is applied to have the capacity to manage dynamic environments. The height observations z_t are modeled using a Gaussian distribution $N(z_t, \sigma_{z_t}^2)$. The height estimate $\hat{h}$ is updated using the observation z_t, taken at time t:

$$\hat{h}(t) = \frac{1}{\sigma_{z_t}^2 + \sigma_{\hat{h}(t-1)}^2} \left(\sigma_{z_t}^2 \hat{h}(t-1) + \sigma_{\hat{h}(t-1)}^2 z_t \right), \tag{4}$$

$$\sigma_{\hat{h}(t)}^2 = \frac{1}{\frac{1}{\sigma_{\hat{h}(t-1)}^2} + \frac{1}{\sigma_{z_t}^2}}. \tag{5}$$

Actually, the new measurements have the main impact. The update is carried out in such a way that the variance of the current estimate is raised with a quantity directly proportional to the time between the previous and the current measurements. A point is rejected from processing if its variance component exceeds a certain value. As a result, highly uncertain information is eliminated [22]. In the next step, a filter is utilized to crop a rectangular area from the height map. The size of the rectangular area is chosen based on the maximum digging reach and the width of the excavator to cover the whole working area.

2.1.2 Kinematics of Excavators

Since the LiDAR sensor is mounted on the top of the excavator to model the front area, the boom, arm, and bucket add extra points to the point clouds that are not representative of the height of the ground. Another challenge is that the positions of these points are not fixed because the boom, arm, and bucket are constantly moving. The extra points should be removed from the obtained point clouds. Firstly, the positions of the revolute joints of the excavator must be estimated, then the points in the proximity of the estimated positions are removed.

In this section, the forward kinematics of an excavator is introduced to estimate the positions of the revolute joints. The motion of the excavator manipulator is described by kinematic equations without taking into account the driving forces and torques. An excavator can be modeled as an open-loop articulated chain with a boom, arm, and bucket. The chain has one end that is free and the other is fixed to a supporting base. In an excavator, a series of rigid bodies, known as links, are joined by revolute joints. When the joint angles are known, the forward kinematic is used to determine the bucket position, whereas the inverse kinematic is utilized to determine the joint angles when the bucket position is known [28]. The kinematics of the excavator is provided in Fig. 4.

Each link has its own Cartesian coordinate system that moves with the link. Most research uses the Denavit-Hartenberg (D-H) convention to manage coordinate transformation between two Cartesian coordinate systems (Tab. 1). The local coordinate system for each link is constructed based on the D-H convention, with the z-axis

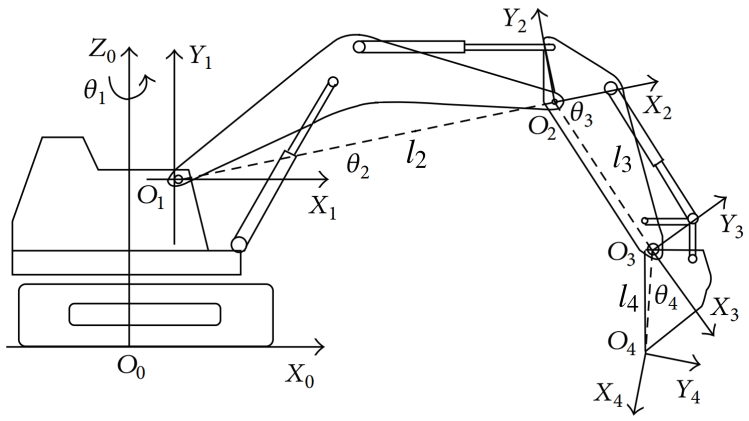

Figure 4: Excavator coordinate systems in Denavit-Hartenberg convention [27].

Table 1: Denavit-Hartenberg parameters [27].

Link$_i$	d_i	a_i	α_i	θ_i
1	0	l_1	90	θ_1
2	0	l_2	0	θ_2
3	0	l_3	0	θ_3
4	0	l_4	0	θ_4

pointing in the direction of rotation of the revolute joint and the x-axis pointing at the other joint in the same link. Therefore, the y-axis direction is established using the right-hand rule. As indicated in Fig. 4, finally given a fixed Cartesian coordinate system is utilized as the machine coordinate system [27].

Forward kinematic equations are utilized to calculate the positions of the manipulator links given the joint angles and lengths of the links. A transformation matrix between two adjacent coordinate systems (from $i+1_{th}$ to i_{th}) on a link can be stated as by using the D-H convention

$$
{}^{i}T_{i+1} = \begin{bmatrix} \cos\theta_{i+1} & -\cos\alpha_{i+1}\sin\theta_{i+1} & \sin\alpha_{i+1}\sin\theta_{i+1} & a_{i+1}\cos\theta_{i+1} \\ \sin\theta_{i+1} & \cos\alpha_{i+1}\cos\theta_{i+1} & -\sin\alpha_{i+1}\sin\theta_{i+1} & a_{i+1}\sin\theta_{i+1} \\ 0 & \sin\alpha_{i+1} & \cos\alpha_{i+1} & d_{i+1} \\ 0 & 0 & 0 & 1 \end{bmatrix} \tag{6}
$$

where θ_{i+1} is the the rotation angle about z_i-axis, α_{i+1} is the rotation angle of z_i-axis about x_{i+1}-axis, d_{i+1} is the offset along the z_i-axis, and a_{i+1} is the length of the link. Any point in any local coordinate system can be shown in the machine coordinate system by the coordinate transformation matrix as

$$
{}^{m}P = {}^{m}T_n\,{}^{n}P = {}^{m}T_1\,{}^{1}T_2\,{}^{2}T_3 \cdots {}^{n-1}T_n\,{}^{n}P, \tag{7}
$$

where ${}^{m}P$ is the position vector in the machine coordinate system, ${}^{m}T_n$ is the transformation matrix from the n_{th} coordinate system to the machine coordinate system, and ${}^{n}P$ is the position vector in the n_{th} coordinate system. In the next step, each link is simply modeled by a cylinder shape. The line passing from two adjacent coordinate systems is the axis of a cylinder. The radius of all cylinders is considered a constant value. The schematic of the modeled boom, arm, and bucket is shown in Fig. 5. The overlapping points between the cylinders and point clouds are removed, and after that, the remaining points are utilized in the elevation terrain mapping algorithm as described earlier. There is no concern if some points that belong to the ground are eliminated since the points are added to the map when the bucket moves away from the ground.

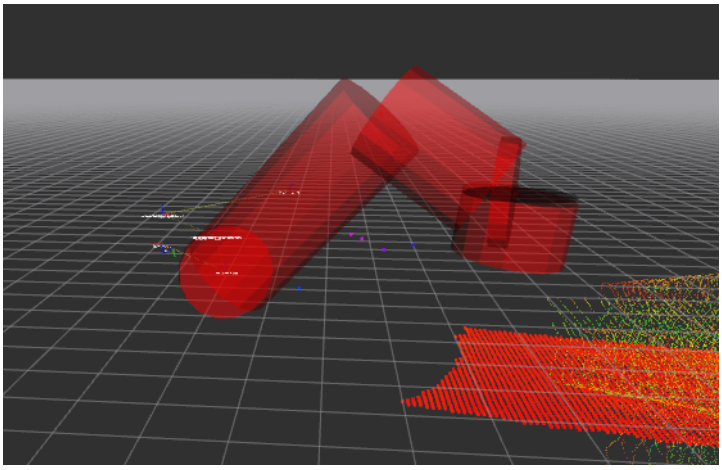

Figure 5: Schematics of the modeled boom, arm, and bucket using cylinders.

2.2 Building information modeling (BIM)

Building information modeling (BIM) is a process that generates and manages digital representations of the physical and functional characteristics of construction projects throughout their life cycle. The model includes detailed information about the project's geometry, construction materials, systems, and other features. Although BIM has

been in the development phase since the 1970s, it didn't become widely accepted until the early 2000s. Nowadays, it is supported by a variety of tools and technologies. The BIM process typically begins with the creation of a 3D model of a construction project and is continually updated throughout the design and construction phases to reflect changes and additions. BIM can be used to visualize the design of a construction project and to simulate how it will function and perform. It can also be used to estimate the cost and time required for a construction project and to identify potential problems or conflicts. BIM is becoming increasingly important in the construction industry as it allows for more accurate and efficient project planning and execution. It can also improve communication and collaboration among project stakeholders and can help to reduce errors and rework [7, 29, 30].

Figure 6: Xsite® PRO 3D system that is installed in the excavator cabin [31].

Novatron Ltd. provides solutions for the robotization of HDMMs and the digitization of construction sites. One of the main products of Novatron Ltd. is Xsite® PRO 3D with LANDNOVA X software that is utilized for model-based construction sites. The Xsite® PRO 3D system is shown in Fig. 6. The Xsite® PRO 3D system is integrated into the BIM and facilitates construction projects. The target 3D models are designed by construction professionals using 3D design software programs, and also, the human operator can design simple models inside the cabin using Xsite® PRO 3D. During the operation, the operator can compare the bucket tip position with the target model using the Xsite® PRO 3D to accurately and rapidly perform the task. In the next step, the 3D-Win® software is utilized to obtain the 3D point cloud of the target model in the desired reference coordinate system with a particular grid size. Finally, the obtained point cloud can be easily utilized in any platform for further investigation [31].

2.3 Productivity Estimation

In this section, an approach for the productivity estimation of an excavator in the grading operation is presented. In the algorithm, firstly, a target model is designed in BIM. Then, when the human operator starts the grading operation, the actual maps from the working areas, which are obtained using the elevation terrain mapping algorithm, are updated every few seconds. Firstly, a region of interest (often abbreviated ROI) is defined around the i_{th} point of the desired model. The ROI is considered a square, and the point is located in the center. The size of the square is equal to the grid size of the target model. In the next step, actual points within the defined ROI should be found. A simple schematic of desired and actual points within the ROI is illustrated in Fig. 7.

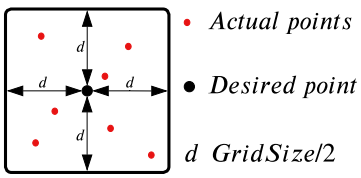

Figure 7: The desired and actual points within the region of interest (ROI).

The actual height is equal to the average height of actual points within the ROI:

$$Z_{Actual} = \frac{\Sigma_{j=1}^{N} z_j}{N}; \quad j \in \{1,2,3,\ldots,N\}, \tag{8}$$

where Z_{Actual} is the average actual height, z_j is the z coordinates of the j_{th} point within the ROI, and N is the total number of points within the ROI. The desired height $Z_{Desired}$ is equal to the z coordinate value of the i_{th}

point in the model. The flowchart of the proposed method is shown in Fig. 8. If a point has not been already marked as a valid point, and the error between the actual and desired height values is less than the threshold, the point is marked as a valid point, and the area of ROI is added to the productivity calculation. Also, when a point has been already accepted as a valid point, we must check the actual height since it might have been changed. When the error exceeds the threshold, the point is marked as an unaccepted point, and the area of ROI must be subtracted from the productivity calculation. In this approach, the productivity might be less than zero which means the error exceeds the threshold. As previously described, in the grading operation the quality of the performed task is highly significant, and this task does not require much adding or removing materials. In the grading operation, the difference between the initial and target surfaces should be smaller than the bucket's height, since when the difference is larger than the bucket's height, the digging operation should be performed before the grading operation.

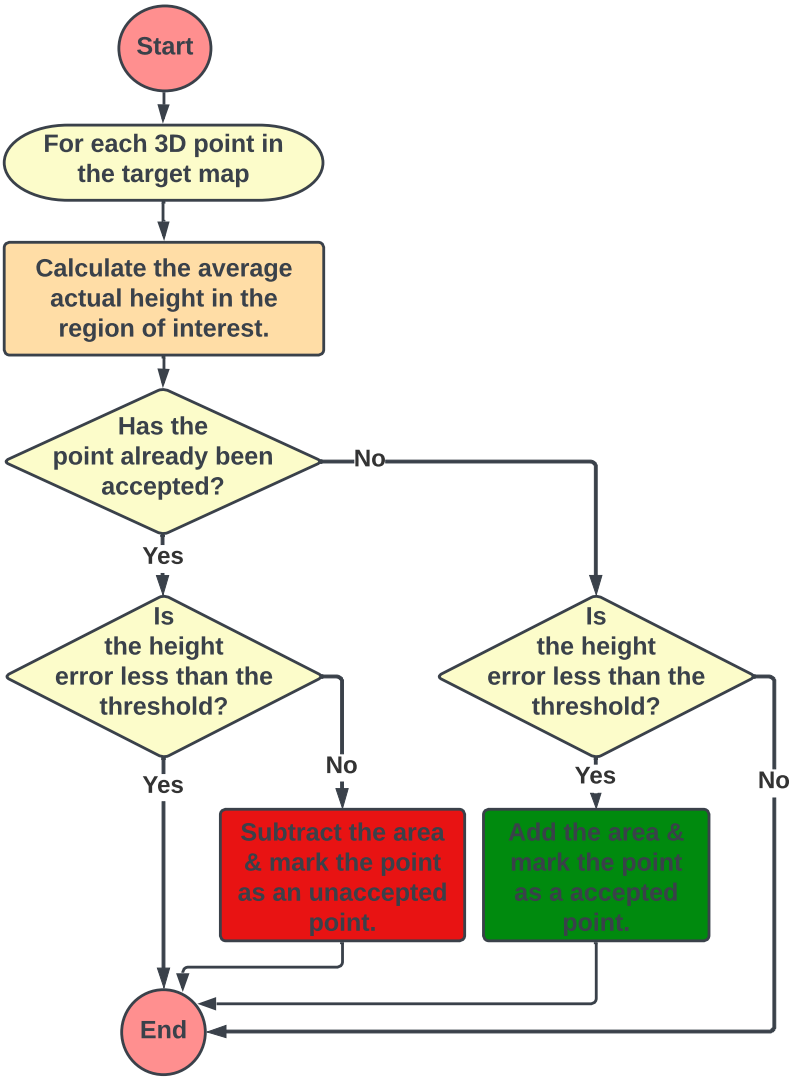

Figure 8: Flowchart of the productivity estimation in the grading operation.

3 Data Collection

In this study, a dataset was collected using a Komatsu® PC138US excavator. Figure 9 shows the crawler excavator utilized in the tests. The excavator is old, but it has been well-maintained because the regular maintenance and inspection have been done every 500 working hours. The excavator has a tiltrotator, and the bucket is attached to the arm using a quick coupler. The heaped bucket capacity based on the Society of Automotive Engineers (SAE) standard is 0.37 m^3. A Livox Horizon LiDAR has been installed on top of the excavator's cabin. The LiDAR

Figure 9: The excavator used in the data collection phase. In the picture, the cabin (1.), boom (2.), arm (3.), and bucket (4.) are highlighted with red boxes [3].

has a wide field-of-view (FOV) of 81.7° horizontally and 25.1° vertically. Data collection took place in a private worksite with no ongoing construction. Actually, there is nothing unanticipated that can stop the operation. In the experiment, the type of material was clay, and a competent operator performed the grading task.

Measurements from the excavator are collected using the MathWorks Simulink® model and Robot Operating System (ROS). The ROS framework enables smooth interoperability between applications created in various languages and executing on various machines [32]. This communication framework enables different parts to have access to different measurements and variables such as the height map and the revolute joints positions. In the experiments, the Simulink® creates and connects its own ROS node to the ROS master in an NVIDIA Jetson AGX Xavier. Figure 10 illustrates the configuration of the IMUs, GNSS, Xsite® PRO 3D, and LiDAR sensor on the excavator. Measurements from the IMUs are transmitted with a sampling frequency of 200 Hz over the controller area network (CAN) bus. A Kvaser leaf light CAN to USB interface is utilized to connect the Simulink® to the CAN bus. Also, the Simulink®, the NVIDIA Jetson AGX Xavier, LiDAR, and GNSS are connected to the ROS network using an Ethernet connection.

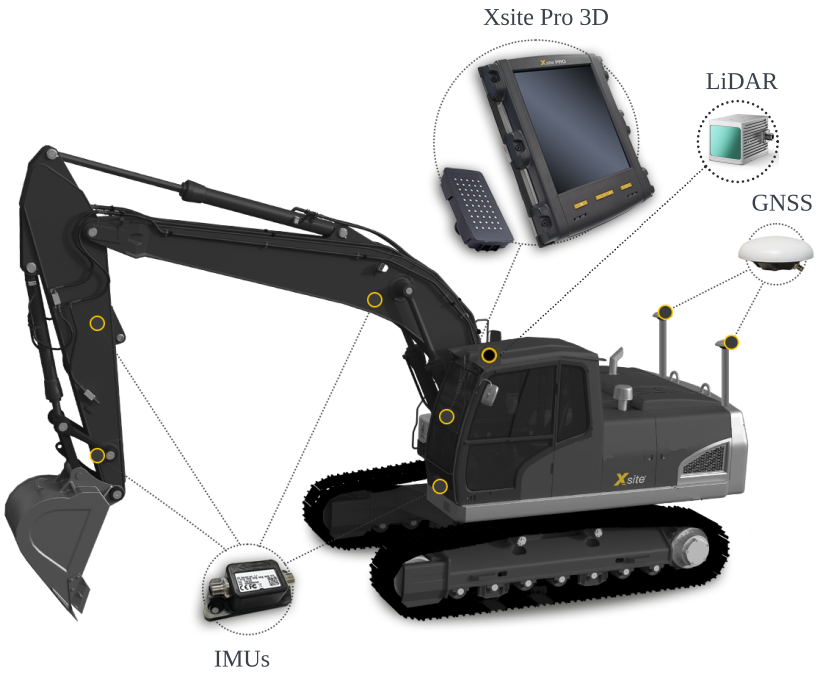

Figure 10: The configuration of the IMUs, GNSS, Xsite® PRO 3D, and LiDAR sensor on the excavator [3].

4 Results

The performance of the suggested method is presented by implementation on the collected dataset. The algorithm is implemented using MathWorks Matlab® R2021a on a laptop with a 1.8 GHz Intel Core i7 CPU and 16 GB of RAM.

Firstly, a target model is designed by the human operator inside the cabin using the Xsite® PRO 3D, and then the 3D point cloud is obtained using the 3D-Win® software. The shape of the desired surface is presented in Fig. 11. The target model is a rectangular surface with a size of approximately 2 $m \times 4$ m. The slopes of the desired surface and the initial terrain are equal to zero, and the depth of the desired surface compared to the initial terrain is equal to 50 cm. In the experiment, the grid size and the required accuracy are equal to 10 cm.

The actual maps from surrounding areas and the productivity estimation are updated every 5 seconds. The productivity of the excavator in the grading operation is presented in Fig. 12. On average, the excavator's productivity in this experiment is approximately 0.02 m^2/sec. This information can be highly useful for worksite managers for future time scheduling and cost analysis. By comparing the metric to industry standards or the productivity of other machines, it is possible to identify project issues and opportunities to improve productivity and increase efficiency.

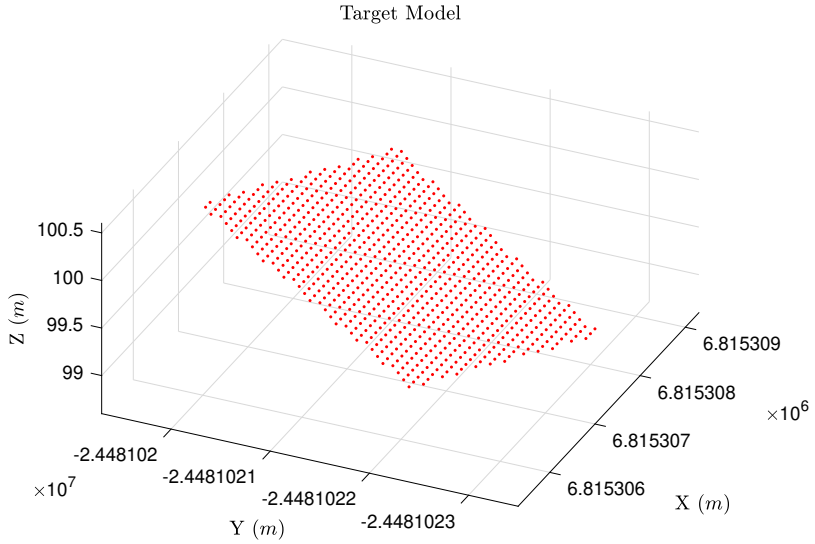

Figure 11: The target model designed in BIM.

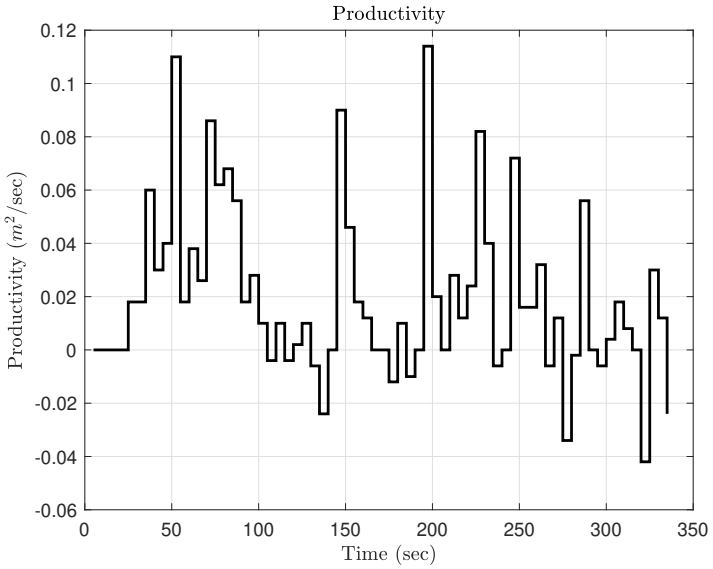

Figure 12: The productivity of the excavator in the grading operation.

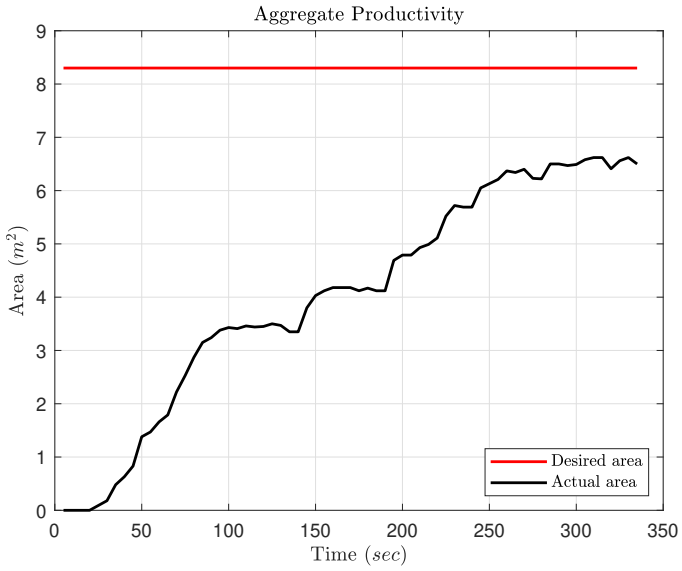

Figure 13: The aggregate productivity of the excavator in the grading operation.

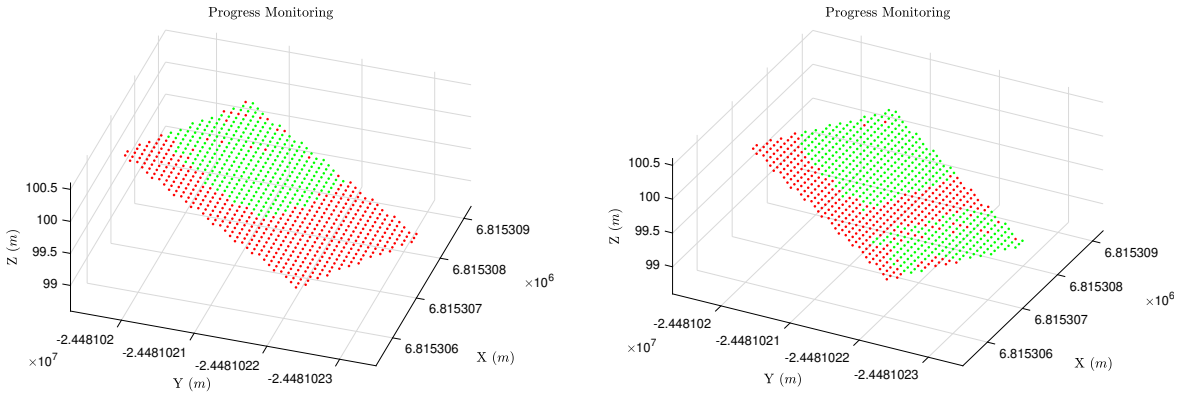

(a) Time = 100 sec

(b) Time = 200 sec

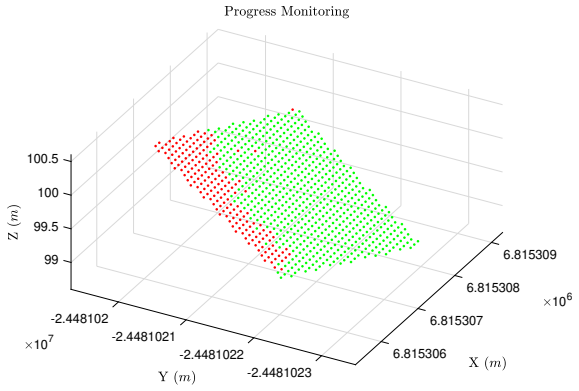

(c) Time = 300 sec

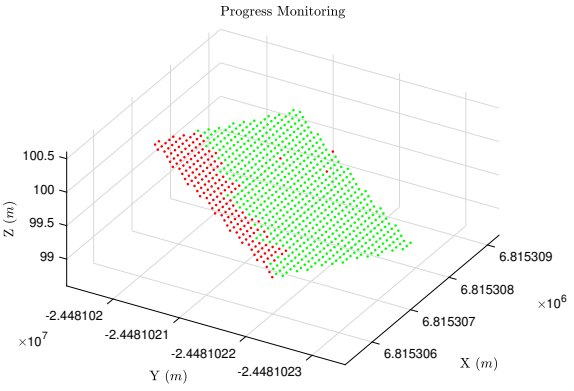

(d) Time = 335 sec

Figure 14: Progress monitoring during the grading operation: (•) green points show the area where the error is less than the threshold, and (•) red points show the area where the error is higher than the threshold.

As you can see, sometimes the productivity estimation is less than zero. Since when the error between the desired and actual height increases to a value higher than the required accuracy, it can cause negative productivity. For instance, it happens when a huge amount of materials fall from the bucket onto a section that is already graded, or

when the bucket goes much in deep, and the error exceeds the limit.

The aggregate productivity of the excavator in the grading operation is illustrated in Fig. 13. At the end of the grading operation, the aggregate productivity is approximately equal to 6.5 m^2 and is less than the total area of the model ($\approx 8.3\ m^2$), because in some sections, the difference between the desired and actual height is more than the required accuracy. Fig. 14 monitors the operation progress at four different times of the operation. The green color shows the section with an error less than the required accuracy, and the red color shows the section with an error higher than the required accuracy. By using the presented method, managers can easily analyze the operation progress, find issues or faults, and then improve the operation. Moreover, human operators can use productivity estimation as feedback to improve their skills and perform the operation with higher accuracy in a shorter time.

5 Conclusion

In this paper, an algorithm is presented to estimate the excavator's actual productivity in the grading operation using building information modeling (BIM). The grading operation is one of the most important and challenging tasks in the worksites that can be performed by excavators. The proposed framework consists of three main parts: (1) elevation terrain mapping algorithm, (2) BIM, and (3) productivity estimation. The grid-based height map is obtained using a LiDAR sensor that is installed on top of the excavator cabin. In the next step, the positions of revolute joints are estimated to be able to remove the extra points which are caused by the movements of the bucket, arm, and boom in front of the excavator. The desired surface is modeled using BIM, and the human operator performs the grading operation based on the target model. In the final step, the excavator's productivity in the grading operation is estimated based on the desired model and obtained map from working areas. The difference between the actual and desired heights must be less than the required accuracy. The presented algorithm is implemented on a dataset collected using an excavator in a private worksite. The results show the method can efficiently monitor the operation progress and productivity. The algorithm can be highly beneficial for construction managers to improve the time scheduling and cost analysis for future operations and projects. Also, human operators can improve their skills using provided productivity estimation. In addition, the proposed method can be utilized to estimate the productivity of automated systems in grading operations. Automated grading systems should have higher productivity compared to manual operations. Furthermore, the presented algorithm can be extended to other common tasks in worksites such as the trenching operation.

Acknowledgement

This project is part of the MORE-ITN project [33], which has received funding from the European Union's Horizon 2020 research and innovation programme under the Marie Skłodowska-Curie grant agreement No 858101.

The MORE project is an innovative European Industrial Doctorate (EID) research and training programme that tries to answer the challenges of HDMMs. The MORE project contributes to the development of state-of-the-art HDMMs by proposing effective solutions driven by digitalization and artificial intelligence (AI). There are eight researchers in the MORE project that work on three main work packages: 1) Process, 2) Machine, and 3) Control. In the process work package, we investigate a set of tasks that are performed by a machine or machines to achieve the purpose of work [33].

We would like to express our deepest gratitude for the continued support of Jari Valtonen, Niko Haaraniemi, and Teemu Mononen in the data collection and analysis steps.

References

[1] Marcus Geimer. *Mobile Working Machines*. SAE International, Warrendale, PA, 2020.

[2] Tyrone Machado, David Fassbender, Abdolreza Taheri, Daniel Eriksson, Himanshu Gupta, Amirmasoud Molaei, Paolo Forte, Prashant Kumar Rai, Reza Ghabcheloo, Saku Mäkinen, et al. Autonomous heavy-duty mobile machinery: A multidisciplinary collaborative challenge. In *2021 IEEE International Conference on Technology and Entrepreneurship (ICTE)*, pages 1–8, Kaunas, Lithuania, August 2021. IEEE.

[3] Amirmasoud Molaei, Marcus Geimer, and Antti Kolu. An approach for estimation of swing angle and digging depth during excavation operation. In *Proceedings of the 39th International Symposium on Automation and Robotics in Construction (ISARC)*, pages 622–629, Bogota, Columbia, July 2022. International Association for Automation and Robotics in Construction (IAARC).

[4] Helen Lingard, Ron Wakefield, and Nick Blismas. If you cannot measure it, you cannot improve it: Measuring health and safety performance in the construction industry. In *the 19th Triennial CIB World Building Congress, Queensland University of Technology,, Brisbane, Queensland, Australia*, 2013.

[5] Chen Chen, Zhenhua Zhu, and Amin Hammad. Critical review and road map of automated methods for earth-moving equipment productivity monitoring. *Journal of Computing in Civil Engineering*, 36(3):03122001, 2022.

[6] Abdullah Rasul, Jaho Seo, and Amir Khajepour. Development of integrative methodologies for effective excavation progress monitoring. *Sensors*, 21(2):364, 2021.

[7] Mohamd Kassem, Elham Mahamedi, Kay Rogage, Kieren Duffy, and James Huntingdon. Measuring and benchmarking the productivity of excavators in infrastructure projects: A deep neural network approach. *Automation in Construction*, 124:103532, 2021.

[8] Mario Klanfar, Vjekoslav Herceg, Dalibor Kuhinek, and Kristijan Sekulić. Construction and testing of the measurement system for excavator productivity. *Rudarsko-geološko-naftni zbornik (The Mining-Geological-Petroleum Bulletin)*, 34(2), 2019.

[9] Caterpillar inc. `https://www.cat.com/en_US/products/new/technology/assist/assist/`. Accessed: 2022-08-01.

[10] Jiaqi Xu and Hwan-Sik Yoon. Sliding mode control of hydraulic excavator for automated grading operation. *SAE International Journal of Commercial Vehicles*, 11(2):113–124, 2018.

[11] Jiaqi Xu, Bradley Thompson, and Hwan-Sik Yoon. Automated grading operation for hydraulic excavators. Technical report, SAE Technical Paper, 2014.

[12] Chang Seop Lee, Jangho Bae, and Daehie Hong. Contour control for leveling work with robotic excavator. *International Journal of Precision Engineering and Manufacturing*, 14(12):2055–2060, 2013.

[13] Jiaqi Xu and Hwan-Sik Yoon. Vision-based estimation of excavator manipulator pose for automated grading control. *Automation in Construction*, 98:122–131, 2019.

[14] Daniel Schmidt, Martin Proetzsch, and Karsten Berns. Simulation and control of an autonomous bucket excavator for landscaping tasks. In *2010 IEEE International Conference on Robotics and Automation*, pages 5108–5113. IEEE, 2010.

[15] Geraldine S. Cheok, Robert R. Lipman, Christopher Witzgall, Javier Bernal, and William C. Stone. Field demonstration of laser scanning for excavation measurement. In *Proceedings of the 17th International Symposium on Automation and Robotics in Construction (ISARC)*, pages 1–6, Taipei, Taiwan, September 2000. International Association for Automation and Robotics in Construction (IAARC).

[16] Xin Zhang and John Morris. Volume measurement using a laser scanner. Technical report, CITR, The University of Auckland, New Zealand, 2005.

[17] J Zico Kolter, Youngjun Kim, and Andrew Y Ng. Stereo vision and terrain modeling for quadruped robots. In *2009 IEEE International Conference on Robotics and Automation*, pages 1557–1564. IEEE, 2009.

[18] Hiroshi Yamamoto, Masaharu Moteki, Takashi Ootuki, Yuji Yanagisawa, Akira Nozue, Takashi Yamaguchi, et al. Development of the autonomous hydraulic excavator prototype using 3-d information for motion planning and control. *Transactions of the Society of Instrument and Control Engineers*, 48(8):488–497, 2012.

[19] Jinhu Wang, Higinio González-Jorge, Roderik Lindenbergh, Pedro Arias-Sánchez, and Massimo Menenti. Automatic estimation of excavation volume from laser mobile mapping data for mountain road widening. *Remote Sensing*, 5(9):4629–4651, 2013.

[20] Hajime Honda, Akifumi Minami, Yoshihiko Takahashi, Seishi Tajima, Takashi Ohtsuki, and Yushi Shiiba. Visualization of the progress management of earthwork volume at construction jobsite. In *Proceedings of the 37th International Symposium on Automation and Robotics in Construction (ISARC)*, pages 1286–1290, Kitakyushu, Japan, October 2020. International Association for Automation and Robotics in Construction (IAARC).

[21] AMAGLO Worlanyo Yao. Volume calculation based on lidar data. Master's thesis, KTH Royal Institute of Technology, School of Architecture and the Built Environment, 2021.

[22] Antti Kolu, Mikko Lauri, Mika Hyvönen, Reza Ghabcheloo, and Kalevi Huhtala. A mapping method tolerant to calibration and localization errors based on tilting 2d laser scanner. In *2015 European Control Conference (ECC)*, pages 2348–2353. IEEE, 2015.

[23] Spherical coordinates system (spherical polar coordinates) newtonian mechanics. https://physicscatalyst.com/graduation/spherical-coordinates-system/. Accessed: 2022-10-21.

[24] Julius Kümmerle, Tilman Kühner, and Martin Lauer. Automatic calibration of multiple cameras and depth sensors with a spherical target. In *2018 IEEE/RSJ International Conference on Intelligent Robots and Systems (IROS)*, pages 1–8. IEEE, 2018.

[25] Adrian Kaczmarek, Witold Rohm, Lasse Klingbeil, and Janusz Tchórzewski. Experimental 2D extended Kalman filter sensor fusion for low-cost GNSS/IMU/Odometers precise positioning system. *Measurement*, 193:110963, 2022.

[26] Alexander Kleiner and Christian Dornhege. Real-time localization and elevation mapping within urban search and rescue scenarios. *Journal of Field Robotics*, 24(8-9):723–745, 2007.

[27] Jiaqi Xu and Hwan-Sik Yoon. A review on mechanical and hydraulic system modeling of excavator manipulator system. *Journal of construction engineering*, 2016, 2016.

[28] Ngoc Tam Lam, Ian Howard, and Lei Cui. *A Review of Trajectory Planning for Autonomous Excavator in Construction and Mining Sites*, pages 368–382. Engineers Australia, BARTON, ACT, 2021.

[29] InfraRYL (general quality requirements for infrastructure construction). https://www.rakennustieto.fi/palvelut/tietoa-rakentamiseen/ryl/infraryl. Accessed: 2022-10-21.

[30] Rauno Heikkiläa, Tanja Kolli, and Teppo Rauhala. Benefits of open Infra BIM - Finland Experience. In *Proceedings of the 39th International Symposium on Automation and Robotics in Construction (ISARC)*, pages 253–260, Bogota, Columbia, July 2022. International Association for Automation and Robotics in Construction (IAARC).

[31] Novatron ltd. https://novatron.fi/en/. Accessed: 2022-02-01.

[32] Morgan Quigley, Ken Conley, Brian Gerkey, Josh Faust, Tully Foote, Jeremy Leibs, and AY Ng. Ros: an open-source robot operating system. ICRA workshop on open source software (vol. 3 no. 3.2), 2009.

[33] MORE-ITN project. https://www.more-itn.eu/. Accessed: 2022-02-01.